Exchange-correlation energy in electron-hole liquid with different electron distributions over the valleys in silicon

V. D. Kulakovskiĭ and I. V. Kukushkin

Institute of Solid State Physics, USSR Academy of Sciences
(Submitted 26 March 1980)
Zh. Eksp. Teor. Fiz. **70**, 1069–1081 (September 1980)

The question is considered of the possibility of stratification into two phases in an electron-hole liquid (EHL) consisting of two electron components and one hole component. It is shown that in the analysis of this problem one cannot neglect the weak dependence of the exchange-correlation energy ε_{xc} on the distribution of the electrons over the valleys. Stratification might be expected in deformed Si if $|\varepsilon_{xc}|$ were to decrease by more than 3% in the case of uniform distribution of the electrons over all six valleys. The emission of a two-electron EHL in Si compressed along the axes ⟨100⟩, ⟨123⟩, and ⟨110⟩ is investigated, and the densities of the "hot" and "cold" electrons are determined. It is found that in all cases $|\varepsilon_{xc}|$ increases by 2–3% when the electrons are uniformly distributed over all six valleys, and no stratification into two phases takes place.

PACS numbers: 71.35. + z, 71.45.Gm

§1. INTRODUCTION

The investigation of an electron-hole liquid (EHL) in a weakly deformed Si or Ge crystal is of particular interest, because in this liquid the electrons from the basis and separated valleys (called respectively "hot" and "cold" electron) are independent components, because of the long intervalley relaxation time.[1-4] We shall use the term "two-electron" for an EHL containing two electron subsystems. Owing to the condition of local electroneutrality, such an EHL is two-component from the thermodynamic point of view. It constitutes the simplest mixture of two quantum Fermi liquids. The energy of a two-electron EHL is a function of two variables, which are conveniently chosen to be the densities of the cold (n_c) and hot (n_h) electrons.

Kirczenow and Singwi[5-6] have recently calculated the phase diagram for a two-electron EHL in Te deformed along the ⟨111⟩ axis (Ge⟨111⟩), starting from the assumption that the exchange-correlation energy ε_{xc} is only a function of the total density $n = n_c + n_h$. Their basic premise that the previously calculated[7,8] values of $\varepsilon_{xc}(r_s)$ in the significant region $r_s = 1-2$ are the same in deformed and undeformed Si and Ge crystal accurate to 3–4% (the dimensionless parameter $r_s = (3/4\pi n)^{1/3} a_B^{-1}$, where a_B is the Bohr radius of the exciton). Kirczenow and Singwi found that the region in which the EHL can be stratified into two phases in Ge⟨111⟩, depends strongly on the effective mass of the holes, which determines the contribution of the kinetic energy of the holes. It follows from the calculations that in Ge⟨111⟩ stratification is possible only at small compressions, when the effective mass of the holes on the Fermi level is large enough. At $T = 0K$, $n_h = 0$ in one phase and $n_h \sim 1/2 n_c$ in the other.

Andryushin, Gel'fond, and Silin[9] calculated $\varepsilon_{xc}(n_h, n_c)$ by the Nozieres-Pines method. They calculated the chemical potential of the cold (μ_c) and hot (μ_h) electron-hole (e-h) pairs in deformed Si and Ge at $n_h/n_c \geqslant 0.3$. According to their calculation, the EHL in Ge⟨111⟩ and Si⟨100⟩ does not stratify at any deformation. We note that the structure of the valence band was taken into account by Andryushin, Gel'fond, and Silin approximately. It follows nevertheless from their work that the calculation of the phase diagram without allowance for the dependence of ε_{xc} on the electron distribution over the valleys is too rough.

The experimentally obtained[1,2] values of μ_h and μ_c in Ge⟨111⟩ were explained by the authors within the framework of the approximation $\varepsilon_{xc} = \varepsilon_{xc}(n)$. More advantageous is an experimental investigation of the two-electron EHL in Si, where the separation of the emission lines in the spectrum and the accuracies of μ_h and μ_c are much better, in view of the larger value of the electron Rydberg (Ry) and hence of the larger energy scales. It follows from the results of Wagner and Sauer[3] that in Si⟨100⟩ the difference $\mu_h - \mu_c$ in an EHL with $n_h/n_c > 0.3$ cannot be described in the approximation $\varepsilon_{xc}(n_c, n_h) = \varepsilon_{xc}(n)$. The question of the possibility of stratification into two phases in a two-electron EHL remains open for both Si and Ge. An investigation into this question, with Si as the example, is the subject of the present paper.

In §3 we present the results of an experimental study of the emission of a two-electron EHL with a ratio $n_h/n_c \lesssim 0.25$ in Si⟨100⟩, Si⟨110⟩, and Si⟨123⟩, and determine the values of μ_h and μ_c. It is precisely this region of the ratios n_h/n_c which is of greatest interest for the investigation of both the dependence of ε_{xc} on the electron distribution over the valleys, and the possibility of stratification of the EHL into two phases. Nonetheless, stratification into two phases was not observed in the EHL.

In §4 we solve for Si the problem of the possibility in principle of stratification of a two-electron EHL both in the $\varepsilon_{xc}(n_c, n_h) \equiv \varepsilon_{xc}(n)$, approximation and when a weak dependence of ε_{xc} on the electron distribution over the valleys is considered. The functions $\mu_h(n_h/n_c)$ and $\mu_c(n_h/n_c)$ are found and it is shown that stratification is possible only if $|\varepsilon_{xc}|$ decreases when the electrons are distributed over all six valleys uniformly within 3–4%. From a comparison of the calculated and measured dependences of μ_h and μ_c and of the EHL density on the ratio n_h/n_c, we find in §5 that $|\varepsilon_{xc}|$ in Si does not decrease but, to the contrary, in-

 0038-5646/80/090543-07$02.40

creases somewhat as $n_h/n_c \to 1$, and the absence of stratification in the two-electron EHL in SI is in full agreement with the calculation.

2. EXPERIMENTAL PROCEDURE

We investigated pure silicon crystal with residual minute impurity concentration (mainly boron) less than 3×10^{12} cm^{-3}. The samples, measuring $1\times3\times10$ mm, were etched prior to each placement in the cryostat in a mixture of fluoric and nitric acids (1 : 3). The procedure of the uniform and uniaxial deformation was described by Kulakovskii, Timofeev, and Edel'shtein.[10] The samples were placed in superfluid helium.

The nonequilibrium carriers were excited either with a pulsed copper-vapor laser ($\lambda = 510.5$ nm, the repetition frequency of the 10-nsec pulses reached 15 kHz, the power in the pulse was 3 kW), or by a cw argon laser with up to 1 W power.

The radiation receiver was a cooled photomultiplier with S-1 cathode, operating in the photon-counting regime. In the case of pulsed excitation, the registration system operated in the strobe-integration regime. The spectral instrument was a double monochromator with a dispersion 10 Å/mm in the working region.

3. RECOMBINATION RADIATION OF EHL IN WEAKLY COMPRESSED SILICON CRYSTALS

In accord with the multiplicity of the conduction-band splitting, two at ($P \| \langle 100\rangle$ and $\langle 110\rangle$) or three ($P \| \langle 123\rangle$) free excitons (FE_i) and e–h pairs in the EHL (L_i) are observed in the emission spectra of weakly compressed silicon (Fig. 1). The intensity ratio of the lines $L_i(I(L_i))$ depended on the conditions of sample surface preparation. In our experiments, $I(L_h)/I(L_c)$ did not exceed 0.25. This ratio characterizes the fraction of

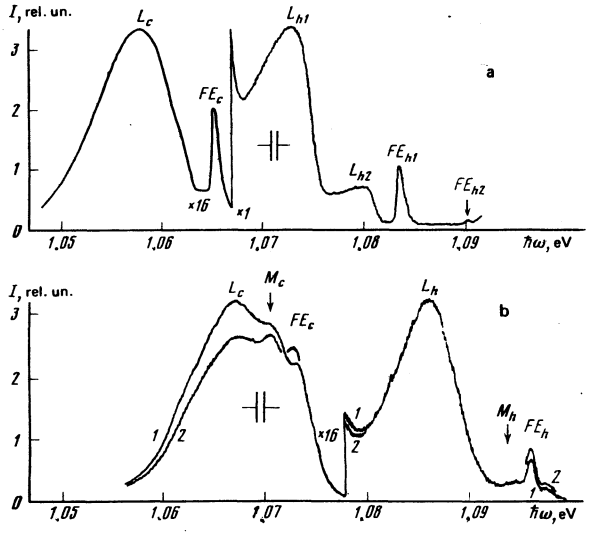

FIG. 1. Emission spectra of Si compressed along the axes $\langle 123\rangle$ and $\langle 100\rangle$ at 2 K (TO component). The spectra of Si $\langle 123\rangle$ were recorded under stationary excitation ($\bar{n} \sim 3.10^{15}$ cm^{-3}), and the spectra of Si $\langle 100\rangle$ (b) under pulsed excitation ($\bar{n} \sim 10^{17}$ cm^{-3}) at a strobe duration 0.15 μsec and at delay times 0 (1) and 0.5 μsec (2), respectively.

the hot electrons in the EHL. We measured the damping times of the line intensities $L_c(\tau_{Lc})$ and $L_h(\tau_{Lh})$ under pulsed excitation of the e–h pairs. It turned out that in all cases ($P \| \langle 100\rangle$, $\langle 110\rangle$, $\langle 123\rangle$) τ_{Lc} and τ_{Lh} differed by not more than 20% at small deformations (Fig. 1, $\tau_{Lh} > \tau_{Lc} \simeq 0.3$ μsec). At these deformation the electron intervalley relaxation time is therefore longer than the e–h pair lifetime. Only when the distances between the lines L_h and L_c exceed the energy of the intervalley TA phonon (~18 meV) does τ_{Lh} decrease rapidly on account of the scattering of the hot electrons by the phonons.

From the form of the EHL emission spectra we determined the chemical potentials of the hot and cold e–h pairs, the equilibrium density $n_0 = n_c + n_h$, and the Fermi energies of the electrons ε_F^i and holes ε_{FH}. It is known[11] that the spectral distribution of the EHL radiation in Si is described in first-order approximation by the expression

$$I(h\nu) \sim \int_{\bullet}^{h\nu} \rho_v[h\nu-\varepsilon]^{1/2} f_e(\varepsilon_F^i, T) f_H(\varepsilon_{FH}, T)\, d\varepsilon, \qquad (1)$$

where $\rho_v(\varepsilon)$ is the state density in the valence band, and $f_e(f_H)$ is the electron (hole) energy distribution function. When the line shape is approximated with the aid of this expression, difficulties arise when it comes to describe the red "tail" of the line L. Therefore, following Ref. 10, we have included in consideration also the broadening of the energy levels below the Fermi level, a broadening characterized by the parameter

$$\Gamma = 0.1\varepsilon_F(1-(\varepsilon/\varepsilon_F)^2).$$

The simplest situation takes place in Si$\langle 123\rangle$, where the splitting ΔE_{c_1} of the valleys c and h_1 in the conduction band is less than the splitting ΔE_v of the valence band, and the L_{h_1} line is still seen in the spectrum at $\Delta E_v = (2-3)\varepsilon_{FH}$. At such high ΔE_v the hole dispersion law is close to quadratic, $\rho_v \sim \varepsilon^{1/2}$. At $n_h/n_c < 0.05$ and $\Delta E_v > 20$ meV the line L_c acquired a canonical form corresponding to $n_0 = (5.5 \pm 0.3)\cdot 10^{17}$ cm^{-3} and to an EHL binding energy $\varphi = -\mathrm{Ry} - \mu_c = 2.3 \pm 0.2$ meV. We call attention to the fact that these values are somewhat higher than in Si$\langle 100\rangle$[$n_0 = (4.8 \pm 0.2)\cdot 10^{17}$ cm^{-3}, $\varphi = 2.0 \pm 0.2$ meV, Ref. 10], in which there are likewise only two valleys in the conduction band but, in contrast to Si$\langle 123\rangle$ the valence band is almost isotropic Therefore, at equal optical masses of the holes, the effective mass of the state density of the holes is 10% larger in Si$\langle 123\rangle$ than in Si$\langle 100\rangle$. As seen from Fig. 2, the density of the excitons, and particularly the biexcitons, is less in Si$\langle 123\rangle$ than in Si$\langle 100\rangle$.

The hot e–h pair emission line L_h in EHL (Fig. 2) has a steep violet edge, in good agreement with the low (≃ 1 MeV) Fermi energy of the hot electrons at $n_h/n_c < 0.1$. When n_h/n_c decreases from 0.25 to 0.01, the violet edges becomes narrower, indicating a decrease of ε_F^h and of the density n_h. If stratification were to take place in the EHL, then n_h and ε_F^h would not change at $n_h/n_c < (n_h/n_c)_{cr}$.

Owing to the inequality $\varepsilon_F^h/\varepsilon_{FH} \ll 1$, the red edge of the L_h line is a measure of the state density of the hole band. Indeed, it is seen from Fig, 2 that in Si$\langle 123\rangle$ at

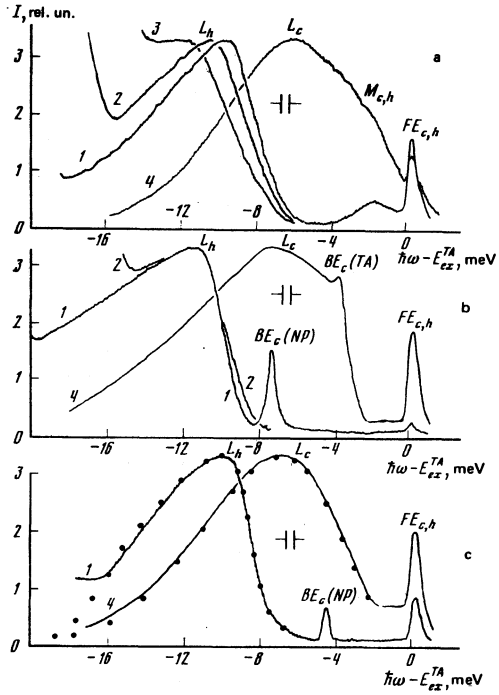

FIG. 2. Comparison of the emission spectra of cold and hot $e-h$ pairs in EHL in Si⟨100⟩ (a), ⟨110⟩ (b) and ⟨123⟩ (c) at 2 K. The lines FE_c and FE_h are superimposed. For curves 1, $(FE_h - FE_c) = 19$, 20 and 18 MeV at P ∥ ⟨100⟩, ⟨110⟩ and ⟨123⟩, respectively. Curves 2 and 3 illustrate the change of the L_h lines when $FE_h - FE_c$ is decreased. Curve 4 in Si⟨100⟩ was obtained under pulsed excitation ($\bar{n} \sim 10^{17}$ cm^{-3}), and the remaining curves under stationary excitation ($\bar{n} \sim 3.10^{15}$ cm^{-3}). The points show the approximation of the lines $L_{c,h}$ in Si⟨123⟩ with the parameters indicated in the table, at $\Gamma = 1.2$ meV. The lines $M_{c,h}$ and BE_c are due to emission of biexcitons and bound excitons, respectively.

$h\nu > 1/4\varepsilon_{FH}$, when the hole level broadening becomes small, $I(h\nu) \sim (h\nu)^{1/2}$. In Si⟨100⟩ and Si⟨110⟩ no such relation is observed, since the hole dispersion law deviates greatly from quadratic, owing to the proximity of the split-off valence band to ε_{FH}.

The violet edge of the $e-h$ pair emission line in an EHL is determined by the value of the chemical potential. If Fig. 2, where the emission lines of the cold and hot excitons are superimposed for convenience, it is seen that $\mu_h < \mu_c$ in all three cases P ∥ ⟨100⟩, ⟨110⟩ and ⟨123⟩. We emphasize that in a two-electron EHL the chemical potentials do not coincide with the average energy on the cold (hot) $e-h$ pair in the EHL. Moreover, the very subdivision into energies of hot and cold $e-h$ pair in such an EHL is indefinite (§4), since the thermodynamic properties of the EHL are determined by the mean energy $\varepsilon(n_c, n_h) = E(N_c, N_h)/(N_c + N_h)$. We note also that at very low ratios ($n_h/n_c \lesssim 0.5$) the hot electrons in the EHL ($T \gtrsim 2$ K) turn out to be nondegenerate ($\varepsilon_F{}^h < 0$). In this case the violet edge $\hbar\omega_v$ of the L_h line "breaks away" from the chemical potential μ_h and remains unchanged with decreasing n_h:

$$\hbar\omega_v = E_g + \mu_h - \varepsilon_F{}^h.$$

A few words concerning the EHL temperature (T_L) in Si. At a sample temperature $T_0 \lesssim 4K$ it is impossible to determine T_L in undeformed silicon from the spectra, since the high Fermi energies of the electrons and holes make the line sharp insensitive to the variation of T_L in the region 2–8 K.[12] The situation is different in the case of hot $e-h$ pairs in EHL, since $\varepsilon_F^h \sim kT$. To find T_L we used the TA components, corrected to account for the spectral width of the gap (~0.3 meV) the TA components of the emission lines L_h and found that in all cases P ∥ ⟨100⟩, ⟨110⟩, and ⟨123⟩, T_L at $T_0 = 2$ K decreased from 6 ± 0.5 K at $P \leq 10$ kG/mm^2 to 4 ± 4.05 K at larger deformations. For Si⟨100⟩ the values of T_L agree with those obtained by Wagner and Sauer.[3] The decrease of the overheating of the EHL with increasing P is apparently due to the decrease of the probability of the radiationless recombination of the $e-h$ pairs in EHL.

If account is taken of the decrease of T_L with increasing deformation, the observed nonmonotonic dependence of $I(FE_c)$ on the deformation becomes understandable. The initial increase of $I(FE_c)$ is due to the decrease of $\varphi = -\mathrm{Ry} - \mu_c$,[10] and the small decrease of $I(FE_c)$ at $P > 15$–20 kG/mm^2, when $\varphi \approx$ const, is due to the decrease of the exciton evaporation from the EHL as a result of the cooling of the latter. The obtained overheating of the EHL compared with T_0 is sufficient to explain the high density of the nonequilibrium excitons in the space between the drops, without resorting to the assumption that the coefficient of sticking of the excitons to the drop is unusually small (<0.04).[13]

The experimentally obtained values $T_L, n_c, \varepsilon_F^c$, $-Ry^c - \mu_c$, $-Ry^h - \mu^h$, $\mu_{xc}^c - \mu_{xc}^h$ are listed in the table. Before we proceed to discuss the experimental results, we consider the thermodynamics of a two-electron EHL.

4. THERMODYNAMICS OF TWO–ELECTRON EHL

To assess the possibility of stratification in a two-electron EHL it is necessary to determine the chemical potentials μ_h and μ_c and the pressure p in the EHL. They are connected with the free energy of the system $F(N_h, N_c, V, T)$ by the relations

$$\mu_i = \left(\frac{\partial F}{\partial N_i}\right)_{N_{j\neq i}, V, T}, \tag{2}$$

$$p = -\left(\frac{\partial F}{\partial V}\right)_{N_h, N_c, T}, \tag{3}$$

where $N_{h(c)}$ is the number of hot (cold) electrons, V is the volume, $i = c$ or h, and the number of holes $N_H = N_c + N_h$, not being an independent parameter, is excluded from consideration. At $T = 0$ the free energy F is equal to the total system energy E

$$E = E_k^h + E_k^c + E_k^H + E_{xc}, \tag{4}$$

where E_k^H, E_k^c, and E_k^h are respectively the kinetic energies of the holes and of the cold and hot electrons, and E_{xc} is the sum of the exchange and correlation energies. At $T = 0$, the values of μ_i and p are

$$\mu_i = \varepsilon_F{}^i + \varepsilon_{FH} + \mu_{xc}{}^i, \tag{5}$$

$$p = p_0{}^h + p_0{}^c + p_0{}^H + p_{xc}, \tag{6}$$

where $\varepsilon_F^i = (\partial E_K^i / \partial N_i)_{V, N_{j\neq i}}$ is the Fermi energy of particles of sort i,

$$\mu_{xc}^{\ i}=\left(\frac{\partial E_{xc}}{\partial N_i}\right)_{V,N_{j\neq i}}, \qquad (7)$$

$$p_0^{\ i}=-(\partial E_{\kappa}^{\ i}/\partial V)_{N_i}, \quad p_{xc}=-(\partial E_{xc}/\partial V)_{N_c,N_h,N}.$$

In the case of simple bands, the calculations of ε_F^i and p_0^i entail no difficulty. To calculate μ_{xc}^i and p_{xc}, however, we must know the dependence of E_{xc} on the total density and on the distribution of the electrons over the valleys. If we assume in first approximation, following Kirczenov and Singwi,[5,6] that $\varepsilon_{xc}\equiv\varepsilon_{xc}(n)$, then

$$\mu_{xc}^{\ c}=\mu_{xc}^{\ h}, \quad \mu_c-\mu_h=\varepsilon_F^{\ c}-\varepsilon_F^{\ h}. \qquad (8)$$

The exchange-correlation energy was taken by us to be the function $\varepsilon_{xc}(n)$, calculated in Ref. 7 for Si compressed along the ⟨100⟩ axis, and to simplify the calculation we approximated it by the analytic expression $-Ar_s^{-3/4}$. At $A=2.55$, the function $\varepsilon_{xc}(r_s)$ calculated by this formula differs in the interval $r_s=1/2-1.8$ from that obtained in Ref. 7 by less than 1%, whereas the difference between $\varepsilon_{xc}(r_s)$ in Si⟨100⟩ and in undeformed Si reaches 2%.[7,8]

The criterion for the stratification of a two-electron EHL is the appearance of a minimum of the function $\mu_h[n_0(x),x]$, where n_0 is the equilibrium density of the e-h pairs in the EHL with a ratio $N_h/N_c=x$.[6] Recognizing that at $T=0$ the gas-phase density is zero, and $n_0(x)$ can be determined from the condition $p[n_0(x)]=0$. The chemical potential $\mu_h(n_0,x)$ is of the form

$$\mu_h=\text{const}\,\frac{(1+x)[x^{2/3}(1-x)-2(\nu_h/\nu_c)^{2/3}-\gamma(1+x)^{5/3}]}{[x+(\nu_h/\nu_c)^{2/3}+\gamma(1+x)^{5/3}]^{4/3}}, \qquad (9)$$

where $\gamma=m_{de}\nu_h^{2/3}/m_{dH}$; $\nu_{c(h)}$ is the number of cold (hot) valleys with effective mass of the state density m_{de}; m_{dH} is the effective mass of the hole state density. The value of μ_h depends on two parameters, ν_h/ν_c and γ. The shaded areas on Fig. 3 show the parameter values at which stratification of the two-electron EHL into two phases is possible. The stratification region depends little on the concrete form of the approximation function for $\varepsilon_{xc}(r_s)$ and can be used for the analysis of the EHL both in Si deformed along various axes, and in Ge. In Si, no stratification of the EHL is possible within the framework of the considered approximation, regardless of the deformation direction. The most favorable situation for stratification is for weakly compressed Ge⟨111⟩, in which, owing to the nonparabolicity of the valence band, the effective state density of the holes near the

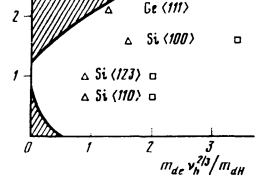

FIG. 3. Region of existence of two-phase EHL in Si and Ge (shaded). The points correspond to the real situation in undeformed (△) and strongly compressed (□) Si and Ge crystals.

TABLE I.

	Si ⟨123⟩	Si ⟨100⟩		Si ⟨110⟩
ΔE_v, meV[1]	21	8.5	12	18.5
n_h/n_e	0.03	0.1	0.06	0.025
$n_0\cdot10^{-17}$, cm^{-3}	5.5±0.3	6.0±0.5	4.8±0.3	7.7±0.3
ε_F^c, meV	4.8±0.2	5±0.4	4.4±0.3	3.8±0.2
$-\mathrm{Ry}^c-\mu_c$, meV	2.3±0.2	3.0±0.3	2.8±0.2	3.8±0.2
$-\mathrm{Ry}^h-\mu_h-\varepsilon_F^h$, meV	9.3±0.3	11.0±0.3	9.0±0.3	10.8±0.3
$-\mu_{xc}^c$, meV[2]	29.9±0.5	31.0±0.8	28.6±0.5	32.3±0.5
$\mu_{xc}^c-\mu_{xc}^h$, meV[2]	2.4±0.4	3.2±0.5	2.8±0.4	3.0±0.4
T, K	5±0.5	7±0.5	5.5±0.5	4±0.5

[1] The quantities ΔE_v were calculated on the basis of the measured splittings of the exciton levels due to the splitting of the conduction band and from the deformation potentials obtained by Lande, Pollak, and Cardona.[14]

[2] In the calculation of μ_{xc}^i, account was taken of the differences between the Ry^i on account of the anisotropy of the conduction and valence bands.

Fermi level is hardly larger than in undeformed Ge.[6]

It is seen from the experimental values of μ_i and ε_F^i (see the table) that the conditions (8) are not satisfied in Si, i.e., the approximation $\varepsilon_{xc}(n_c,n_h)\equiv\varepsilon_{xc}(n)$ is crude. We now attempt to ascertain the role of the weak dependence of ε_{xc} on the electron distribution over the valleys. Since we are interested only in the small region $r_s=1.2-1.7$, we can approximate $\varepsilon_{xc}(r_s)$ at a fixed ratio n_h/n_c by using functions of the type Ar_s^{-k} with two adjustment parameters A and k. As noted above, in this range of r_s the calculated $\varepsilon_{xc}(r_s)$ dependences, both in underformed and in uniaxially compressed Si and Ge (Refs. 7, 9) can be approximated by functions of the type $-Ar_s^{-k}$ with an error less than 1%. From the calculations of $|\varepsilon_{xc}^{(\nu)}(r_s)|$ it follows that with increasing number ν of valleys this function decreases somewhat at small r_s and increases at large ones. In the limit of a large number of valleys ($\nu\sim100-1000$)$\varepsilon_{cx}^{(\nu)}(r_s)$ (Ref. 15) intersects with $\varepsilon_{xc}^{(1)}(r_s)$ at $r_s=r_{sx}=0.05$. The functions $\varepsilon_{xc}(r_s)$ in Si⟨100⟩ (2 valleys) and in undeformed Si (6 valleys) intersect according to the calculations[7,8] at $r_{sx}=1.4$ (Fig. 4), but the error in the determination of r_{sx} on the basis of these calculations is large.

For the case of two types of carrier, it is convenient to choose the arguments in ε_{xc} to be r_s and the variable

$$y=\left(\frac{n_c}{\nu_c}-\frac{n_h}{\nu_h}\right)\left(\frac{n_c}{\nu_c\Delta_c}+\frac{n_h}{\nu_h\Delta_h}\right)^{-1}, \qquad (10)$$

where the parameters Δ_c and Δ_h reflect the nonequivalence of the limiting cases with $n_h=0$ and $n_c=0$ at $\nu_h\neq\nu_c$, $\Delta_h=\Delta_c$ at $\nu_h=\nu_c$. Since ε_{xc} depends little on n_c-n_h, we confine ourselves to the first terms of the Taylor expansion of $\varepsilon_{xc}(r_s,y)$ and write $\varepsilon_{xc}(r_s,y)$ in the following form, which is convenient for calculations:

$$\varepsilon_{xc}(r_s,y)=\varepsilon_{xc}^{(\nu_c+\nu_h)}(r_s)(r_{sx}/r_s)^{f(y)}, \qquad (11)$$

where $\varepsilon_{xc}^{(\nu_c+\nu)}=-Ar_s^{-k}$ and $f(y)\ll1$, r_{sx} is the point of intersection of the curves $\varepsilon_{xc}^{(\nu_c+\nu_h)}(r_s)$ and $\varepsilon_{xc}^{(\nu_c)}(r_s)$. Since it follows from experiment that $\mu_{xc}^h-\mu_{xc}^c$ varies monotonically with increasing $|y|$, the function $\varepsilon_{xc}(r_s,y)$ should also vary monotonically with increasing $|y|$. We chose $f(y)=y^m$, where the parameter $m>1$ because of the condition that $\mu_{xc}^{c,h}$ must be continuous at $y=0$. From

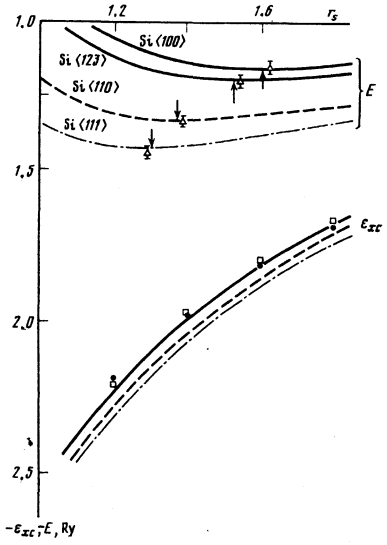

FIG. 4. Exchange correlation energy ε_{xc} and average energy E of $e-h$ pairs in EHL in uniaxially compressed Si at $\nu=2$ (solid line), $\nu=4$ (dashed), and $\nu=6$ (dash-dot). $\varepsilon_{xc}^{(2)}=-2.55\, r_s^{-0.717}$; $\varepsilon_{xc}^{(4)}=-2.60\, r_s^{-0.709}$; $\varepsilon_{xc}^{(6)}=-2.632\, r_s^{-0.702}$. The calculated and experimental values of r_{s0} and E are indicated by arrows and triangles, respectively. The $\varepsilon_{xc}(r_s)$ dependences in Si ⟨100⟩ and in undeformed Si, calculated in Refs. 7 and 8, are shown respectively by squares and points.

(10) and (11) it follows that the change of $\varepsilon_{xc}^{(\nu)}$ is

$$\delta\varepsilon_{xc}^{(\nu_c+\nu_h\to\nu_{c(h)})}\equiv\varepsilon_{xc}^{(\nu_c+\nu_h)}-\varepsilon_{xc}^{(\nu_{c(h)})}\approx\varepsilon_{xc}^{(\nu_h+\nu_c)}\Delta_{c(h)}^{m}\ln(r_s/r_{sx}),$$

$$\delta\varepsilon_{xc}>0 \text{ at } r_s<r_{sx} \text{ and } \delta\varepsilon_{xc}<0 \text{ at } r_s>r_{sx}.$$

In Si⟨123⟩, when the two upper valleys are empty, we have $\nu_c=\nu_h=2$ and $\Delta_c=\Delta_h=\Delta$. For the equilibrium density $r_{s0}(y)$ we obtain from the condition $p=0$

$$r_{s0}(y)=\left\{\frac{\alpha[(1-y/\Delta)^{5/3}+(1+y/\Delta)^{5/3}+2^{5/3}\gamma)}{2^{2/3}A(k+y^m)r_{sx}^{ym}}\right\}^{1/(2-k-ym)}, \qquad (12)$$

where $\alpha=2.21m_{ex}/m_{de}\nu_h^{2/3}$, m_{ex} is the reduced mass of the exciton. In Si⟨123⟩ we have $\alpha=0.5316$, $\gamma=2.00$, $m_{ex}=0.1228m_0$. From (7) we obtain for μ_{xc}^{i}

$$\mu_{xc}^{i}(r_s,y)=\varepsilon_{xc}(r_s,y)[1+(k+y^m)/3+(y\pm1)m\Delta y^{m-1}\ln(r_s/r_{sx})], \qquad (13)$$

where the upper and lower signs are for μ_{xc}^{h} and μ_{xc}^{c}, respectively.

The values of Δ, m, and r_{sx} can be determined from the conditions of the best fit of the functions $r_{s0}(y)$ and $\mu_{c,h}(y)$(§5) and those calculated from (12) and (13) (§5). For the time being we shall stop to discuss some general consequences. The equality $\mu_{xc}^{c}=\mu_{xc}^{h}$ is violated at $\Delta\neq0$. The sign of the difference $\delta\mu_{xc}=\mu_{xc}^{h}-\mu_{xc}^{c}$ coincides with the sign of $\delta\varepsilon_{xc}^{(4\to2)}$:

$$\delta\mu_{xc}[r_{s0}(y),\ y]=2m\Delta y^{m-1}\varepsilon_{xc}(r_{s0}(y),\ y)\ln(r_{s0}(y)/r_{sx}). \qquad (14)$$

An analysis of the functions $\mu_{xc}^{i}(n_h/n_c)$ has shown that the region in which stratification in the EHL is possible, which was obtained above in the approximation $\varepsilon_{xc}(r_s,y)\equiv\varepsilon_{xc}(r_s)$ (Fig. 3) broadens at $\delta\varepsilon_{xc}^{(\nu_h+\nu_c\to\nu_c)}>0 (r_{s0}<r_{sx})$ and narrows down at $\delta\varepsilon_{xc}^{(\nu_h+\nu_c\to\nu_c)}<0$. Figure 5a illustrates the effect of the $\varepsilon_{xc}(y)$ dependence on the possibility of stratification in Ge⟨111⟩. At $\delta\varepsilon_{xc}^{(4\to1)}>0$ the minimum on the $\mu_h(r_s,y)$ curve becomes deeper (curve 3), and at

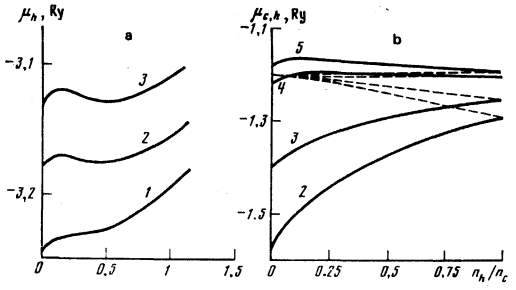

FIG. 5. The functions $\mu_h(n_h/n_c$ in Ge⟨111⟩ (a) and Si⟨123⟩ (b (solid lines and $\mu_c(n_h/n_c)$ in Si⟨123⟩ (b) (dashed) at various values of $\delta\varepsilon_{xc}/\varepsilon_{xc}$: 0.015 (1); 0 (2); −0.02 (3); −0.047 (4); −0.053 (5).

$\delta\varepsilon_{xc}^{(4\to1)}<0$ it becomes shallower and vanishes entirely if $\delta\varepsilon_{xc}^{(4c\to1)}/\varepsilon_{xc}^{(4)}>0.015$ (curve 1). The absolute change of μ_h on going from curve 2, calculated under the assumption $\varepsilon_{xc}(n_c,n_h)\equiv\varepsilon_{xc}(h)$, to curve 1 amounts in this case to only 0.2 meV, which is within the limits of the errors in the determination of μ_h from the emission spectra. Thus, agreement, within the limits of the measurement errors, between μ_{xc}^{h} and μ_{xc}^{c} in Ge⟨111⟩ can not serve as the basis for the applicability of the approximation $\varepsilon_{xc}(n_c,n_h)\equiv\varepsilon_{xc}(n)$.

We consider now the conditions under which stratification of the EHL in Si⟨123⟩ would be possible. Since there is no stratification within the framework of the approximation $\varepsilon_{xc}(n_c,n_h)\equiv\varepsilon_{xc}(n)$, it is necessary that $|\varepsilon_{xc}|$ decrease when the electrons are uniformly distributed over all the valleys ($r_{sx}>r_{s0}$). Figure 5b shows plots of $\mu_{c,h}(n_h/n_c)$ for Si⟨123⟩ at various parameters Δ and at $m=2$. Curves 2, 3, 4, and 5 correspond to a relative decrease of $|\varepsilon_{xc}|$, i.e., to $\delta\varepsilon_{xc}^{(4\to2)}/|\varepsilon_{xc}^{(4)}|$ respectively equal to 0, 2, 4.7 and 5.3%.

In the first two case stratification is still impossible, in the third it already takes place, with n_h/n_c in phase equal to n_c/n_h in the other. At $\delta\varepsilon_{xc}^{(4\to2)}/|\varepsilon_{xc}^{(4)}|=0.053$ the electrons from different valleys are not mixed at all in the EHL, and for any n_h/n_c it should be stratified into two, one containing only hot electrons and the other only cold. We note that so large values of $\delta\varepsilon_{xc}^{(4\to2)}/|\varepsilon_{xc}^{(4)}|$ are not realistic, inasmuch as it follows from earlier studies[10-12] that no stratification of the EHL takes place in Si with equivalent values.

5. DISCUSSION OF EXPERIMENTAL RESULTS FOR SILICON

It follows from the obtained chemical potentials and Fermi energies of cold and hot electrons and holes (see the table) that in Si compressed along any of the axes ⟨100⟩, ⟨110⟩, and ⟨123⟩ we have $\mu_{xc}^{h}<\mu_{xc}^{c}$ at $n_h/n_c<0.25$. Therefore the fact that there is no stratification in the EHL is in full agreement with the conclusions obtained in the preceding section. This result agrees also with the calculation of Andryushin, Gel'fond, and Silin[9] for EHL in Si⟨100⟩ with $n_h/n_c\geq0.3$.

On the basis of the measured experimental functions $\mu_{c,h}(n_h/n_c)$ and $r_{s0}(n_h/n_c)$, within the framework of the approximation considered in §4, we can reconstruct the

change in the exchange-correlation energy when the electrons become distributed over different valleys. The valleys of $\mu_{c,h}(n_h/n_c)$ and $r_{s0}(n_h/n_c)$ at $n_h/n_c<0.25$ were obtained from the emission spectra of the two-electron EHL in Si⟨123⟩ (§3), while $\mu_{c,h}$ and r_{s0} at $n_h/n_c=1$ (the electrons uniformly distributed over the four valleys) can be taken from the results of measurements on Si strongly compressed along the ⟨110⟩ axis, since the effective masses of the state densities in the valence bands of Si⟨123⟩ and Si⟨110⟩ agree within 0.2% ($m_{dH}^{\langle 123\rangle}=0.2563$, $m_{dH}^{\langle 110\rangle}=0.2568$) and the electrons in Si⟨110⟩ are located in four valleys.

To find the two parameters A_2 and k_2 in the function $\varepsilon_{xc}^{(2)}(r_s)=-A_2r_s^{-k_2}$ we have two experimental values of μ_c and r_{s0} at $n_h=0$. The best agreement is reached at $A_2=2.55$ and $k_2=0.717$. We note that the obtained $\varepsilon_{xc}^{(2)}(r_s)$ dependence almost coincides with that obtained in Ref. 7 (Fig. 4). To reconcile the calculated function $\delta\mu_{xc}(n_h/n_c)$ with the experimentally obtained one we must set $m=2$ and $\Delta^2\ln(r_{s0}/r_{sx})=0.023$. When these values change by more than 20%, the calculated dependences go beyond the framework of the experimental errors. We note that

$$\Delta^2\ln\left(\frac{r_{s0}}{r_{sx}}\right)\approx\frac{\delta\varepsilon_{xc}^{(4\to2)}(r_{s0})}{\varepsilon_{xc}^{(4)}(r_{s0})}.$$

The change $\delta\varepsilon_{xc}^{(4\to2)}$ thus amounts to only $2.3\pm0.4\%$.

If one fixes the value $\Delta^2\ln(r_{s0}/r_{sx})=0.023$, then r_{sx} can be varied in the wide range from 0.1 to 0.6 (Fig. 6). If, however, it is assumed in accord with the calculations of Refs. 7 and 8 that $r_{sx}=1.4$, then r_{s0} at $n_h=n_c$ and $\delta\mu_{xc}$ as $n_h\to0$ cannot be described simultaneously. In particular, if we fix $\delta\mu_{xc}$, then the $r_{s0}(n_h/n_c)$ dependence does not agree with the measurements even qualitatively (Fig. 6).

In Si compressed along the axes ⟨100⟩ ($\nu_h=4$, $\nu_c=2$) and ⟨110⟩ ($\nu_h=2$, $\nu_c=4$), is expressed by the single formula

$$\varepsilon_{xc}(r_s,y)=\varepsilon_{xc}^{(6)}(r_s)(r_{sx}/r_s)^{y^2}. \tag{15}$$

It follows from (15) and (16) that

$$\varepsilon_{xc}^{(\nu_c,h)}(r_s)=\varepsilon_{xc}^{(6)}(r_s)(r_{sx}/r_s)^{\Delta_{c,h}^2}, \tag{16}$$

$$\delta\varepsilon_{xc}^{(6\to\nu_c,h)}\sim\Delta_{c,h}^2\ln(r_s/r_{sx}). \tag{17}$$

As $n_h/n_c\to0$ we can obtain from (7) and (15)

$$\delta\mu_{xc}=2\frac{\nu_c}{\nu_h}\delta\varepsilon_{xc}^{(6\to\nu_c)}\left[1+\left(\frac{\delta\varepsilon_{xc}^{(6\to\nu_c)}}{\delta\varepsilon_{xc}^{(6\to\nu_h)}}\right)^{1/2}\right]. \tag{18}$$

Since $\delta\mu_{xc}\sim\delta\varepsilon_{xc}/\nu_h$, addition of almost "empty" valleys, as expected, does not lead to a strong change of $\delta\mu_{xc}$. This result agrees well with the observed value of $\delta\mu_{xc}$ on going from Si⟨123⟩ to Si⟨100⟩ (see the table).

From the experimental values of $\delta\mu_{xc}$ as $n_h/n_c\to0$ in Si⟨100⟩ and Si⟨123⟩ we find that $\delta\varepsilon_{xc}^{(6\to2)}(r_{s0})=-1.1\pm0.2$ meV and $\delta\varepsilon_{xc}^{(6\to4)}(r_{s0})=-0.46\pm0.1$ meV or $\delta\varepsilon_{xc}^{(6\to2)}/\varepsilon_{xc}^{(4)}=0.038\pm0.004$, $\delta\varepsilon_{xc}^{(6\to4)}/\varepsilon_{xc}^{(4)}=0.018\pm0.004$. Their difference agrees well with the previously obtained value $\delta\varepsilon_{xc}^{(4\to2)}/\varepsilon_{xc}^{(4)}=0.023\pm0.004$.

Assuming that the points of intersection of $\varepsilon_{xc}^{(2)}(r_s)$, $\varepsilon_{xc}^{(4)}(r_s)$ and $\varepsilon_{xc}^{(6)}(r_s)$ coincide, we obtained

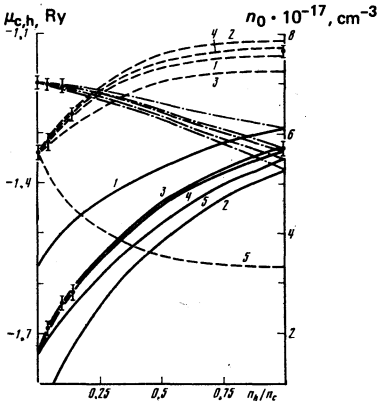

FIG. 6. Plots of μ_h (solid lines), μ_c (dash-dot), and n_0 (dotted) against the ratio n_h/n_c in Si ⟨123⟩, calculated at $m=2$ and at various parameters ($\delta\varepsilon_{xc}/\varepsilon_{xc}$), Δ and r_{sx}: 1—$\delta\varepsilon_{xc}/\varepsilon_{xc}=0$; 2—$\delta\varepsilon_{xc}/\varepsilon_{xc}=0.041$; $\Delta^2=0.015$, $r_{sx}=0.1$; 3—5 —$\delta\varepsilon_{xc}/\varepsilon_{xc}=0.023$, Δ^2 and r_{sx} are respectively equal to: 3—0.023; 0.55, 4—0.0083; 0.1; 5—0.244; 1.4. Points—experimental values.

$\varepsilon_{xc}^{(6)}(r_s)=-2.632r_s^{-0.702}$. The calculated values of the equilibrium density and binding energy $n_0=9.5\cdot10^{17}$ and $\varphi=5.3$ meV (Fig. 6) in Si strongly compressed along the ⟨111⟩ axis, when there are six equivalent valleys in the conduction band, agree well with the earlier experimental values[10] $n_0=(9.8\pm0.3)\cdot10^{17}$ cm^{-3} and $\varphi=5.5\pm0.2$ meV.

Thus, investigations of two-electron EHL in Si make it possible to determine the average exchange-correlation energy with increasing number of valleys. No stratification of the EHL into two phases takes place in Si. It follows from the foregoing analysis, however, that $\delta\mu_{xc}$ depends little on the number ν_h and stratification can take place in semiconductors with $cm_{de}\nu_c^{2/3}/m_{dH}\lesssim1$ and with a sufficiently large number of hot valleys ν_h.

[1]H.-h. Chou, G. K. Wong, and B. J. Feldman, Phys. Rev. Lett. **39**, 959 (1977).
[2]G. J. Feldman, H.-h. Chou, and G. K. Wong, Sol. State Comm. **28**, 305 (1979).
[3]J. Wagner and R. Sauer, Phys. Stat. Sol. (b) **94**, 69 (1979).
[4]B. J. Feldman, H.-h. Chou, and G. K. Wong, Sol. State Comm. **26**, 209 (1978).
[5]G. Kirczenow and K. S. Singwi, Phys. Rev. Lett. **41**, 326 (1978); **42**, 1004 (1979).
[6]G. Kirchenow and K. S. Singwi, Phys. Rev. **B19**, 2117 (1979); **B20**, 4171 (1979).
[7]P. Vashishta, P. Bhattacharyya, and K. S. Singwi, Phys. Rev. **B10**, 5108 (1974).
[8]P. Bhattacharyya, V. Massida, K. S. Singwi, and P. Vashishta, Phys. Rev. **B10**, 5127 (1974).
[9]E. A. Andryushin, O. A. Gel'fond, and A. P. Silin, Fiz. Tverd. Tela (Leningrad) **22**, 1418 (1980) [Sov. Phys. Solid State 22, 827 (1980)].
[10]V. D. Kulakovskiĭ, V. B. Timofeev, and V. M. Édel'shteĭn, Zh. Eksp. Teor. Fiz. **74**, 372 (1978) [Sov. Phys. JETP **47**, 193 (1978)].
[11]J. Hensel, T. G. Phillips, and G. A. Thomas, Solid State Physics (F. Seitz, D. Turbull, and H. Ehrenreich, eds.), Academic, 1978, Vol. 32, p. 88.
[12]A. F. Dite, V. D. Kulakovskiĭ, and V. B. Timofeev, Zh. Eksp. Teor. Fiz. **72**, 1156 (1977) [Sov. Phys. JETP **45**, 604

(1977)].
[13]R. B. Hammond and R. N. Silver, Phys. Rev. Lett. 49, 523 (1979).
[14]L. D. Laude, F. H. Pollak, and M. Cardona, Phys. Rev. B3, 2623 (1971).
[15]E. A. Andryushin, V. S. Babichenko, L. V. Keldysh, T. A. Onishchenko, and A. P. Silin, Pis'ma Zh. Eksp. Teor. Fiz. 24, 210 (1976) [JETP Lett. 24, 185 (1976)].

Translated by J. G. Adashko

Surface oscillations of a Fermi liquid

Yu. B. Ivanov

I.V. Kurchatov Institute of Atomic Energy, Moscow
(Submitted 1 April 1980)
Zh. Eksp. Teor. Fiz. 79, 1082–1094 (September 1980)

Surface oscillations of a normal Fermi liquid are analyzed using the Landau phenomenological theory. A scheme is formulated for describing surface effects using a kinetic equation with a self-consistent field; this scheme is based on successive separation of surface parts of various characteristics of a liquid. Boundary conditions on a free surface are derived. An expression is obtained for the surface tension. Oscillations of a Fermi liquid are studied under hydrodynamic and collisionless conditions and the distributions of the density and current in the presence of such oscillations are found.

PACS numbers: 62.10. + s

1. INTRODUCTION

Khodel' *et al.*[1,2] used the Fermi liquid approach[3] at absolute zero to develop a theory of surface oscillations of a Fermi liquid and they applied this theory to nuclear vibrational states. The theory describes successfully low collective nuclear states but considerable difficulties are encountered in the derivation of simple analytical expressions in the macroscopic limit of a large system such as liquid ^{3}He. It is important to stress that this approach does not require formulation of any boundary conditions on the free surface of a liquid. Fomin[4] formulated a scheme for describing surface phenomena in the collisionless case on the basis of a kinetic equation with a self-consistent field and certain boundary conditions on the free surface: the condition of specular reflection of quasiparticles and the ordinary hydrodynamic boundary condition with surface tension. Therefore, it would be interesting to investigate how these boundary conditions appear in a more general approach and also to describe surface phenomena not only in the collisionless case but also allowing for collisions.

Our aim is to develop a simply quasiclassical theory of surface oscillations of a normal Fermi liquid describing the dynamics of this liquid in the hydrodynamic and collisionless cases, and capable of dealing with surface phenomena in liquid ^{3}He. We shall use the Landau phenomenological theory of a Fermi liquid.[5] We shall formulate a description of surface phenomena using a kinetic equation with a self-consistent field. We shall derive boundary conditions on the free surface and these will be identical, apart from unimportant corrections, with the conditions used by Fomin.[4]

We shall obtain an expression for the surface tension which will be somewhat approximate: it will not include the quantum term arising because of the nonlocality of the relationship between the density of the system $\rho_0(\mathbf{r})$ and the self-consistent field $U_0(\mathbf{r})$ (Refs. 1 and 2). This occurs because of quasiclassical description given by a kinetic equation gives a poor description of the surface where $\rho_0(\mathbf{r})$ and $U_0(\mathbf{r})$ rapidly vary with the coordinates. However, the quasiclassical approach holds very well in the interior of a large system if $k \ll p_F$ (k is the oscillation wave vector and p_F is Fermi momentum) and it describes the dynamics of surface oscillations. Thus, all the inaccuracy of the quasiclassical approach reduces to the inaccuracy in the calculation of just one theoretical constant which is the surface tension.

We shall consider oscillations of a Fermi liquid in the hydrodynamic and collisionless case and find the distributions of the density and current in the presence of such oscillations. In the hydrodynamic case ($\omega\tau \ll 1$) the spectrum of surface waves is identical with the spectrum of capillary waves in viscous hydrodynamics, which is to be expected, and the motion of the liquid is described by laws of hydrodynamics. In the collisionless case ($\omega\tau \gg 1$), we shall show that there are two surface branches. The first low-lying branch is a continuation of a capillary hydrodynamic branch and is found to be simply damped. The second higher branch is a quantum analog of the Rayleigh surface waves in a solid[6] and it is considered in detail in Fomin's paper.[4] This second branch exists only if the constant in front of the first harmonic of the effective interaction is $F_1 > 6$, i.e., if transverse zero sound can travel in the system.

Application of the results obtained to liquid ^{3}He shows that both capillary and Rayleight oscillations are strongly damped in ^{3}He under collisionless conditions.

 0038-5646/80/090549-06$02.40